

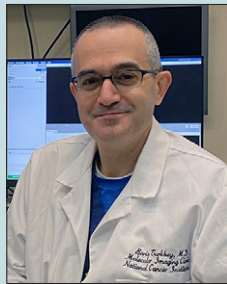
# Deep Learning Unveils Hidden Angiography in Noncontrast CT Scans

Ran Zhang, PhD • Baris Turkbey, MD

**Dr Ran Zhang** is an assistant professor in the Department of Radiology at the University of Wisconsin–Madison. His research focuses on the applications of artificial intelligence in radiography and CT. He also has an interest in the development of artificial intelligence models for triage, diagnosis, and risk stratification. He is a member of the American Association of Physicists in Medicine and serves as an associate editor for *Medical Physics*.



**Dr Baris Turkbey** is a senior clinician at the Molecular Imaging Branch (MIB), National Cancer Institute, National Institutes of Health. He currently serves as the head of MRI and Artificial Intelligence Resource sections at MIB. He is a fellow of the Society of Abdominal Radiology and a member of the PI-RADS Steering Committee. His main research areas include cancer imaging (MRI, PET/CT), quantitative imaging biomarkers, and translational artificial intelligence.



**C**T angiography (CTA) is a widely used diagnostic imaging technique to visualize blood vessels and assess vascular conditions. Iodinated contrast agents are commonly used in CTA to enhance the visibility of vascular structures and facilitate the diagnosis of vascular conditions such as aneurysms, dissections, and atherosclerosis. However, iodinated contrast agents can also lead to adverse effects in patients, including both anaphylactoid and nonanaphylactoid reactions (1). Environmentally, these agents pose long-term concerns as they can contaminate water sources after being excreted through urine (2). The recent shortage in contrast media due to pandemic-related supply chain issues also raises alarm, given the ever-growing number of CT examinations performed using contrast agents. Thus, there could be meaningful clinical and ecological impact if a method for generating synthetic CTA images from noncontrast CT images was developed and used for certain diagnoses.

From the perspective of the computer vision field, the task of generating synthetic CTA images from noncontrast CT images can be framed as an image-to-image translation problem. This encompasses a broad spectrum of applications in medical imaging, ranging from image quality enhancement (eg, denoising and super resolution) to translation between different imaging modalities

(eg, MRI to CT). The incorporation of deep learning methods, particularly generative adversarial networks (GANs), has greatly accelerated progress in this area. The conditional GAN (3), a specific GAN architecture, is particularly useful for this task as it comprises a generator and a discriminator. In the context of synthetic CTA image generation, the generator can accept a noncontrast CT image and generate a synthetic CTA image. The discriminator is trained to compare synthetic CTA images to real CTA images and determine whether the synthetic CTA images look real or fake. In the training process, the generator model is trained to both fool the discriminator and minimize the difference between the synthetic CTA image and the real CTA image. The conditional GAN has had tremendous success in general image-to-image translation tasks based on evaluations of whether the generated samples look realistic to humans. However, two important questions arise regarding the task of synthesizing CTA images: First, is there sufficient information to differentiate blood and soft tissues in noncontrast CT images to enable translation into synthetic CTA images? Second, can the synthetic CTA images match the diagnostic accuracy of real CTA images?

In this issue of *Radiology*, Lyu and Fu and colleagues (4) explore the use of a GAN-based deep learning model to generate synthetic CTA images of the neck and abdomen from noncontrast CT scans. To address the first question, the authors compared Hounsfield unit values in different vascular regions of aortic aneurysms in noncontrast CT images. They observed small but nonnegligible differences in Hounsfield units between blood and the surrounding tissues, which aligns with findings from another study (5). To evaluate the image quality of synthetic CTA images, the authors examined quantitative image quality metrics including normalized mean absolute error, peak signal-to-noise ratio, and the structural similarity index measure. Additionally, two senior radiologists rated the visual quality of three features using a three-point scale: vessel wall clarity, lumen edge sharpness, and lumen wall contrast. They also assessed the diagnostic accuracy of the synthetic CTA images for aortic and carotid artery diseases such as aneurysm, dissection, and atherosclerosis.

Lyu and Fu and colleagues trained their GAN-based CTA imaging (CTA-GAN) model using paired noncontrast CT and CTA scans from 1749 patients from one institution. Scans from 1137 patients were used for training, 400 for validation, and 212 for internal testing. An external

From the Department of Radiology, University of Wisconsin–Madison, Madison, Wis (R.Z.); and Molecular Imaging Branch, National Cancer Institute, National Institutes of Health, 10 Center Dr, Room B3B85, Bethesda, MD 20892 (B.T.). Received October 14, 2023; revision requested October 23; revision received October 26; accepted October 27. Address correspondence to B.T. (email: [turbeyj@mail.nih.gov](mailto:turbeyj@mail.nih.gov)).

Conflicts of interest are listed at the end of this article.

See also the article by Lyu and Fu et al in this issue.

Radiology 2023; 309(2):e232784 • <https://doi.org/10.1148/radiol.232784> • Content codes: **HN CT** • © RSNA, 2023

This copy is for personal use only. To order copies, contact [reprints@rsna.org](mailto:reprints@rsna.org)

test data set including 42 patients from another institution was also used. In the proposed CTA-GAN model, the authors introduced a corrector alongside the generator and discriminator. This corrector accounts for the misregistration between the paired noncontrast and CTA images and is jointly trained with the generator and discriminator. Two discriminators were employed to account for both global and local (central vascular region) image features. The authors compared the CTA-GAN model with two other conditional GANs used for image-to-image translation: pix2pix and RegGAN. In quantitative evaluations, the CTA-GAN model achieved a normalized mean absolute error of 0.013, a peak signal-to-noise ratio of 31.58, and a structural similarity index measure of 0.906 in the external test set, values that were all better than those of the other GAN variants. In the visual quality assessment, over 95% of the synthetic CTA images generated in both the internal and external test sets received a high-quality score overall and for the three individual visual features, with no evidence of a difference in quality observed between real and synthetic CTA images ( $P$  value range, .18 to >.99). For diagnostic accuracy evaluation in the external test set, the synthetic CTA images demonstrated 100% sensitivity and 97% specificity for aneurysms, 67% sensitivity and 100% specificity for dissections, 87% sensitivity and 89% specificity for atherosclerosis, and 100% sensitivity and 95% specificity for healthy arteries. The overall accuracy for the synthetic images was 86%, with a macro F1 score of 0.83.

The use of GAN models to synthesize CTA images from noncontrast CT images has also been explored in other studies. In one study (5), the authors trained a CycleGAN model—which is a type of GAN designed for unpaired image-to-image translation—on an abdominal aortic aneurysm data set composed of 75 patients and evaluated the quantitative image quality, aneurysm lumen segmentation accuracy, and thrombus spatial morphology classification accuracy using the synthetic CTA images. Instead of using the full axial CT section as input, the authors used image patches surrounding the aorta as input to the model. They achieved 86.1% accuracy for aneurysm lumen segmentation and 93.5% accuracy for thrombus spatial morphology classification. In another study (6), the authors proposed an aorta-aware GAN for abdominal aortic aneurysm detection, employing scans from a small cohort of 26 patients for training and internal testing. They achieved an F1 score of 0.85 for aneurysm detection. Both studies used a relatively small training data set compared with this study.

One limitation of this study is the small size of the external test set. As shown in this work, the accuracy of the model dropped from 94% in the internal test set to 86% in the external test set. However, this discrepancy may be attributed to the notably smaller size of the external test set. It is essential to have a large external test set with patients from a targeted population,

so that the diagnostic accuracy of the model can be reliably evaluated. It is also important to evaluate how sensitive the model is to different CT systems and scanning parameters, as the drop in accuracy on the external test set could be related to such factors. Finally, given the 95% specificity for healthy arteries in both the internal and external test sets, representing a 5% rate of missed diagnoses, it is vital to clearly define the intended use of this tool and the appropriate patient population for its reliable and responsible use.

Nevertheless, this work further demonstrates the feasibility of generating synthetic CTA images from noncontrast CT images using deep learning and establishes the baseline diagnostic accuracy of the method for several vascular diseases. Recent advances in the field of generative modeling, particularly the development of diffusion models (7,8), might present alternative model architectures for this task and potentially enhance performance compared with current GAN variants (9). There is also potential to expand the scope of the CTA-GAN model developed by Lyu and Fu and colleagues to even smaller vessels and include more pathologies. However, when new technologies are introduced, it remains essential to train and validate the model using well-curated clinical data sets and perform clinically relevant evaluations, as was done in this work.

**Disclosures of conflicts of interest:** R.Z. No relevant relationships. B.T. Cooperative research and development agreements with NVIDIA and Philips; royalties from the National Institutes of Health; and patents in the field of artificial intelligence.

## References

1. Singh J, Daftary A. Iodinated contrast media and their adverse reactions. *J Nucl Med Technol* 2008;36(2):69–74; quiz 76–77.
2. Dekker HM, Stroomberg GJ, Prokop M. Tackling the increasing contamination of the water supply by iodinated contrast media. *Insights Imaging* 2022;13(1):30.
3. Mirza M, Osindero S. Conditional generative adversarial nets. arXiv 1411.1784 [preprint] <https://arxiv.org/abs/1411.1784>. Published November 16, 2014. Accessed October 5, 2023.
4. Lyu J, Fu Y, Yang M, et al. Generative adversarial network-based noncontrast CT angiography for aorta and carotid arteries. *Radiology* 2023;309(2):e230681.
5. Chandrashekar A, Handa A, Lapolla P, et al. A deep learning approach to visualize aortic aneurysm morphology without the use of intravenous contrast agents. *Ann Surg* 2023;277(2):e449–e459.
6. Hu T, Oda M, Hayashi Y, et al. Aorta-aware GAN for non-contrast to artery contrasted CT translation and its application to abdominal aortic aneurysm detection. *Int J Comput Assist Radol Surg* 2022;17(1):97–105.
7. Song Y, Sohl-Dickstein J, Kingma DP, Kumar A, Ermon S, Poole B. Score-based generative modeling through stochastic differential equations. arXiv 2011.13456 [preprint] <https://arxiv.org/abs/2011.13456>. Published November 26, 2020. Updated February 10, 2021. Accessed October 5, 2023.
8. Ho J, Jain A, Abbeel P. Denoising diffusion probabilistic models. In: Larochelle H, Ranzato M, Hadsell R, Balcan MF, Lin H, eds. *Advances in neural information processing systems 33 (NeurIPS 2020)*. Red Hook, NY: Curran Associates, 2020;33:6840–6851.
9. Dhariwal P, Nichol A. Diffusion models beat GANs on image synthesis. In: Ranzato M, Beygelzimer A, Dauphin Y, Liang PS, Wortman J, eds. *Advances in neural information processing systems 34 (NeurIPS 2021)*. Red Hook, NY: Curran Associates, 2021;34:8780–8794.